Journal of Structural Geology, Vol. 6, No. 6, pp. 639 to 654, 1984
Printed in Great Britain

0191-8141/84 $03.00 + 0.00

Flow stresses from microstructures in mylonitic quartzites of the Moine Thrust zone, Assynt area, Scotland

A. ORD* and J. M. CHRISTIE

Department of Earth and Space Sciences, University of California at Los Angeles, Los Angeles, CA 90024, U.S.A.

(*Received* 4 *May* 1983; *accepted in revised form* 28 *December* 1983)

Abstract—Recrystallized grain sizes, subgrain sizes and dislocation densities of quartz grains in quartzose mylonitic rocks have been examined using optical and transmission electron microscopy (TEM). The samples come from the Moine Thrust zone in the Assynt district, Scotland. They had been studied previously and described in detail with respect to their structural position in relation to the various thrusts in the region and to their preferred orientation. Stresses were derived from these samples using empirical and theoretical equations relating flow stress to the scale of the microstructures. The stresses determined, 43–244 MPa from recrystallized grain size, 9–13 MPa from etched subgrain size, 50–95 MPa from TEM-scale subgrain size and 75–147 MPa from dislocation density, are not constant in individual samples. Simultaneous formation of the quartz fabrics and of the dynamically recrystallized grains during the period of mylonitization may have occurred under flow stresses ranging from 43 to 244 MPa. A later dynamic recovery event reset subgrain sizes and dislocation densities to a constant value for each microstructure throughout the area. There is insufficient empirical information available on the flow stress/subgrain size relationship and on the effects of annealing recovery and annealing recrystallization to allow for a more detailed interpretation. Recrystallized grain size is still the most easily measured microstructural feature and the relationship of recrystallized grain size to flow stress has a sounder experimental basis than subgrain size or dislocation density. The effect of chemical environment on the behaviour of all the microstructures is still unknown.

INTRODUCTION

RECRYSTALLIZATION commonly accompanies deformation by dislocation creep in the crust and upper mantle of the earth. In metallurgy such behaviour, known as 'hot-working', occurs for materials deformed at temperatures greater than half their absolute melting temperature (McQueen & Jonas 1975, p. 394). It has been found that the sizes of subgrains and recrystallized grains and the density of dislocations are sensitive to and equilibrate with flow stress during such high temperature flow of metals, alloys, ceramics and some minerals (for reviews of the metallurgical literature, see Bird *et al.* 1969, McQueen & Jonas 1975, Takeuchi & Argon 1976). The aim of this study is to apply similar relationships observed in experimentally deformed quartz aggregates to microstructures in natural tectonites in order to infer geological flow stresses.

In this study, dislocation density, subgrain size and recrystallized grain size have been measured in quartz mylonites from a major fault zone, that of the Moine Thrust in the Assynt district, Scotland. The structural positions of the specimens used in relation to the various thrusts in the region, their preferred crystallographic orientations, and the timing of formation of the petrofabrics with respect to the phases of deformation represented in this region have already been studied and described by Christie (1963). The present detailed study of the microstructures can be compared with the earlier work to see if all the information is compatible within and between specimens with respect to their history. Furthermore, the microstructures of the naturally deformed rocks can be compared with those of the experimentally deformed rocks from which the relationships of dislocation density and of recrystallized grain size to flow stress used in this study were derived.

The same techniques were used by the same operators for measurement of the microstructures in both the naturally deformed and the experimentally deformed rocks. The experiments were conducted with the aim of examining the microstructure vs flow stress relationships important for the interpretation of mylonite zones; and it is inferred from the similarities between all the microstructures that the flow mechanisms operating in the experiments were dominant also in the formation of the Assynt quartz mylonites. More confidence can therefore be placed in this application of empirical relationships to natural rocks than in previous studies.

The geographic and geologic settings and the petrographic characteristics of the specimens will be described first to provide a basis for the present study. The microstructures have been studied in more detail than previously and the flow stress/microstructure relationships are also different from those used earlier, so the relevant background information will be summarized. Finally, the results of this study will be analysed with a view to determining the style and timing of the various events which resulted in the observed microstructures and to relating the microstructures to the known periods of deformation in the region. An additional aim is to determine flow stresses for the events. This analysis

* Present address: Department of Earth Sciences, Monash University, Clayton, Victoria 3168, Australia.

highlights the lack of experimental information on the behaviour of quartz and quartzites during and after deformation.

REGIONAL STUDY—THE MOINE THRUST ZONE, ASSYNT AREA, SCOTLAND

Geological setting

The Moine Thrust carries the Moine schists of the central and northern Highlands of Scotland over Cambrian, Ordovician and Torridonian sedimentary rocks and Lewisian gneiss. It trends NNE to SSW (Fig. 1, insert) across the northwest coastal region of Scotland. Its surface trace is approximately straight except for an embayment in the north known as the 'Assynt bulge' or the 'Assynt culmination' where the field relations of the Sole, Glencoul, Ben More and Moine Thrusts are best exposed (Peach *et al.* 1907). The concentration of research in this area since the turn of the century (see Christie 1963, for a review up to the mid-1950s, and Elliott & Johnson 1980, for more recent research) has clarified most aspects of its geology. To the north and south of the Assynt bulge, the Moine thrust is found to overlap all underlying thrust sheets to bring the Moine schists in contact with the undisturbed foreland succession. Displacement on the Moine thrust has been considered to range from a minimum of 10 km (Christie 1963, p. 411) to about 100 km (Elliott & Johnson 1980, p. 95).

Mylonitic rocks are developed both above and below the surface mapped as the Moine Thrust (Christie 1963, p. 358) and involve most of the rocks of the foreland succession (Elliott & Johnson 1980). Metamorphic assemblages within this area are characteristic of the greenschist facies (Christie 1960, p. 87).

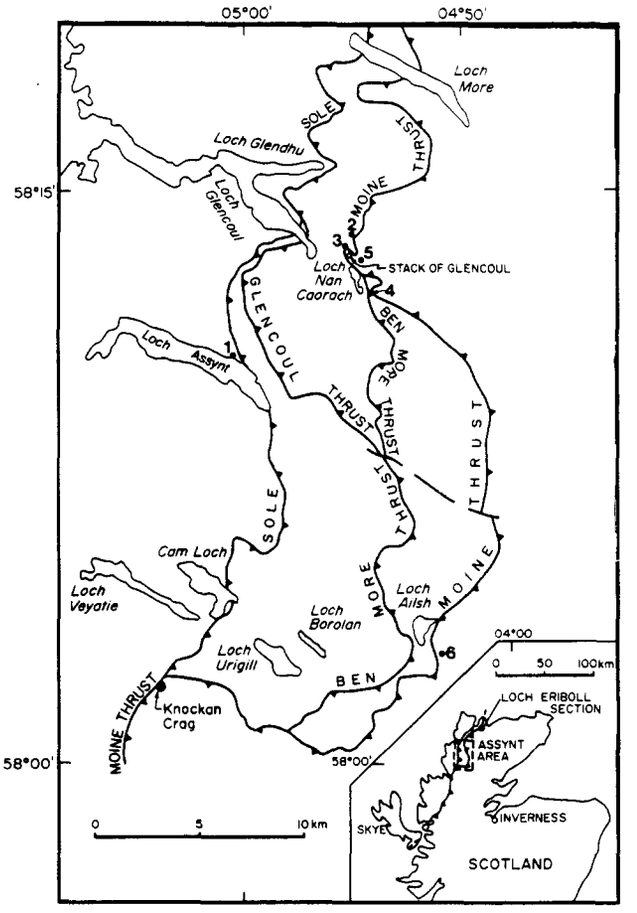

Fig. 1. Location map for Assynt area, Scotland, is insert to map showing localities of the quartzite specimens analysed in this study and the major structural units of the Assynt area (after Christie 1963). Traces of thrust faults show teeth on the hanging wall.

Geographic and structural locations of specimens

The localities of the six specimens examined in this study are shown in Fig. 1. The field maps showing these localities are in the possession of JMC. Specimen 1 is the only representative in this suite of the undeformed foreland quartzites. It comes from a section of gritty and current-bedded Cambrian basal quartzite west of the thrust belt and is regarded here as the relatively undeformed equivalent of the mylonitic quartzites described below. The deformed Cambrian basal quartzite immediately below the Moine Thrust is represented by specimens 2 to 4. Specimen 2 was collected about one km north of the Stack of Glencoul; specimen 3 about 30 m west of the Stack; and specimen 4, due east of the Ben More Thrust from the south end of Loch nan Caorach. These specimens come from areas affected only by the ESE-plunging (B) system of small folds (Christie 1963, p. 359, figs. 4 and 22). Proximity to the line marked as the Moine Thrust increases upwards from specimen 1 to specimen 4. Specimen 5 comes from a zone of redeformed Moine schists and mylonites lying above the Moine Thrust about 500 m east of the Stack of Glencoul, near the Glencoul River, where the mylonite zone has been displaced by later movement on the Ben More Thrust. This sample contains one of the late N-plunging folds (B_n) characteristic of this zone (Christie 1963, p. 363). Specimen 6 comes from a lens of deformed quartzite in the mylonitic rocks above the thrust, on Allt nan Sleagh (Christie 1963, p. 369, fig. 10). It also is in a region containing only the early ESE-trending folds and lineations (B).

Specimen descriptions

The specimens are pure quartzites which display the complete range of microstructures associated with the quartz mylonites of the Moine Thrust. An orthoquartzite is deformed, with elongation of relict grains accompanied by increasing undulatory extinction and the development of deformation lamellae, subgrains and recrystallized grains, to an entirely recrystallized quartz mylonite.

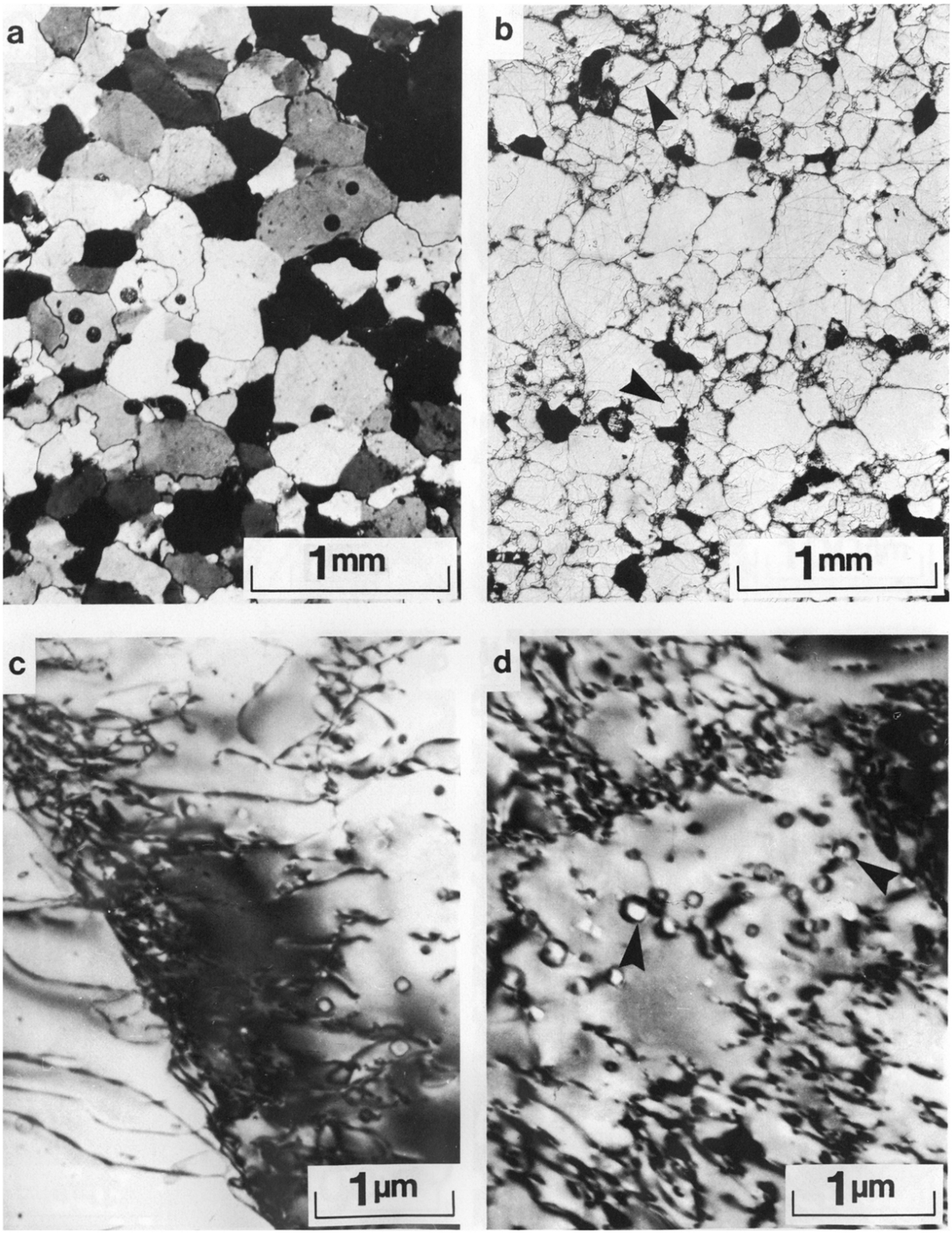

Fig. 2. Specimen 1, undeformed foreland orthoquartzite. (a) Transmitted light photomicrograph taken between crossed polarizers (XPL). (b) Reflected light photomicrograph in plane-polarized light (PPL) of a polished and etched surface displaying well-delineated grain boundaries. Arrows point to Dauphiné twin boundaries. Black areas are hollows from which grains fell out during the polishing and etching procedures. Fine criss-crossing lines are polishing scratches. (c) A cell boundary of tangled dislocations runs NW–SE across this TEM image. (d) Arrows point to equant voids which are commonly associated with dislocations (TEM).

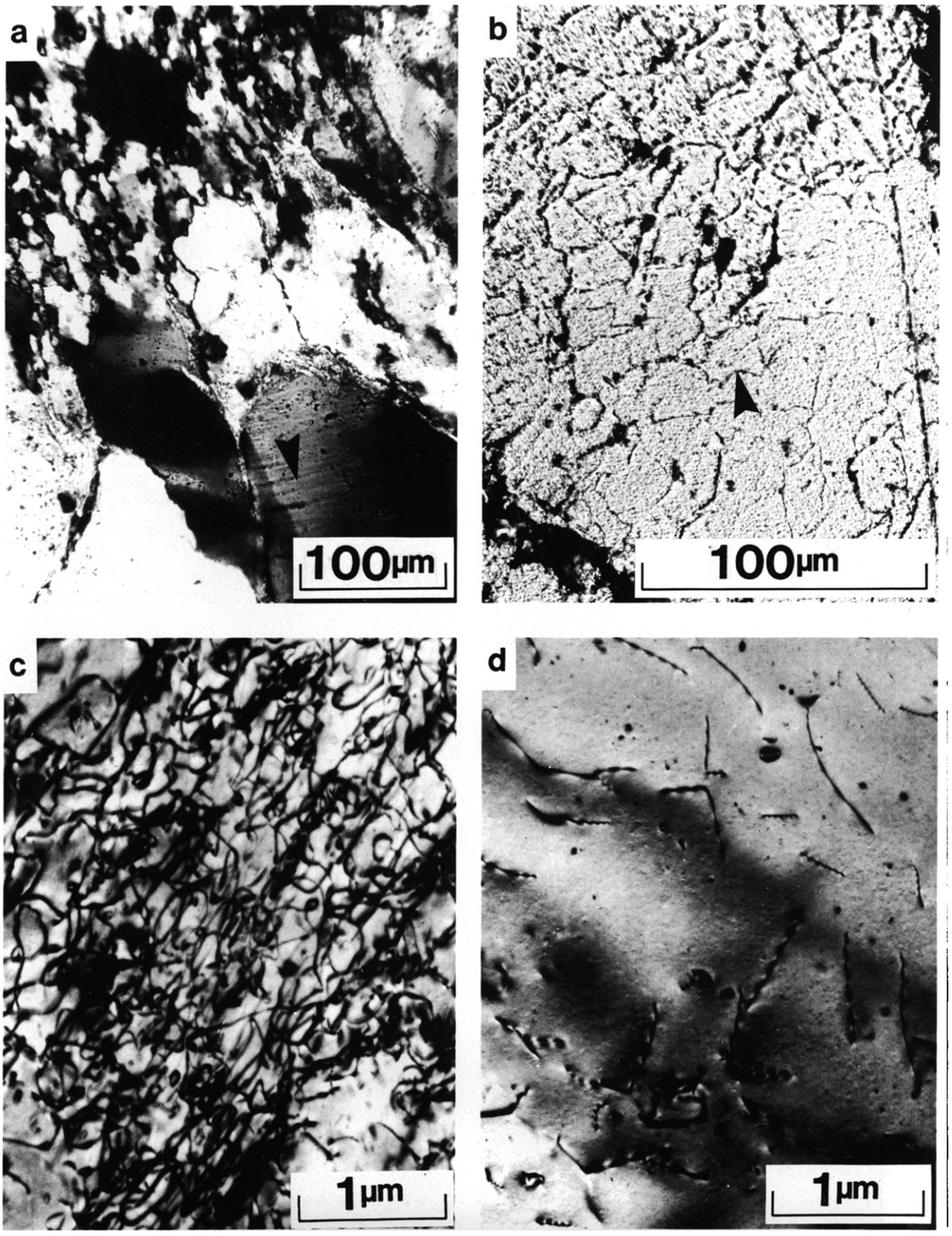

Fig. 3. Specimen 2, deformed Type I quartzite. (a) Transmitted light photomicrograph (XPL) showing relict grains in SE corner; recrystallized grains in NW corner. Note slight NW–SE elongation of grains, undulose extinction and subgrains within relict grains, and arrow pointing to deformation lamellae. (b) Reflected light photomicrograph (PPL) of an etched surface of a relict grain displaying a well-developed subgrain structure. Arrow points to a subgrain boundary. (c) High density of tangled, curved and looped dislocations, too tangled and dense to count in this TEM image. (d) Lower density of dislocations, approximately 5×10^8 cm^{-2} (TEM).

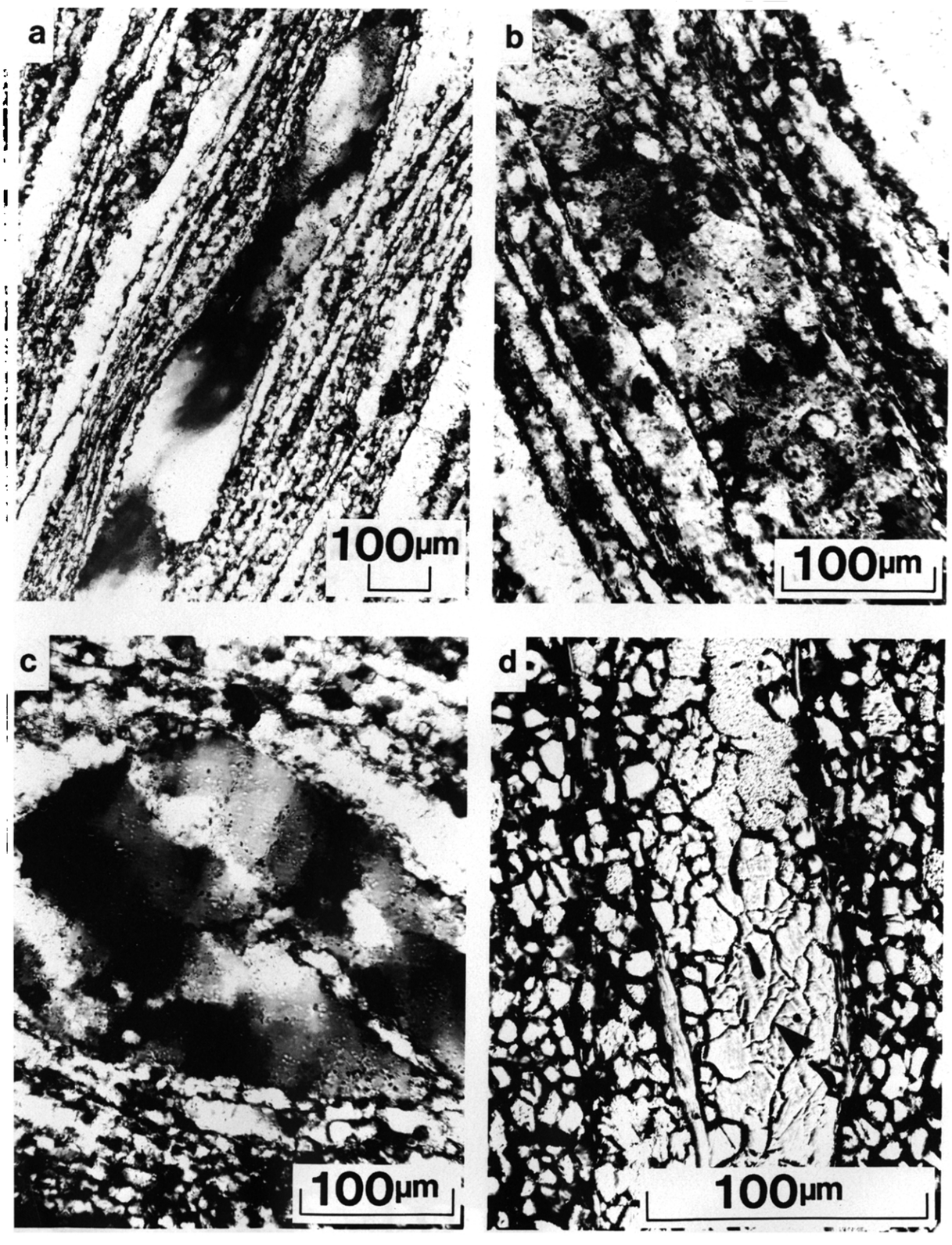

Fig. 4. Specimen 3, further deformed Type I quartzite. (a) Transmitted light photomicrograph (XPL). Deformation bands at a slight angle to the length of this boudinaged relict quartz grain (NE–SW) are progressively misoriented outward from its centre. Subgrain development within the relict grain is best seen at the necked region just above centre. The ribbons of recrystallized grains which lie parallel to the relict grain may each represent originally single quartz grains. (b) Transmitted light photomicrograph (XPL). The central region (NW–SE) represents a relict quartz grain displaying a well-developed subgrain structure. It is surrounded by equigranular recrystallized quartz grains of approximately the same size as the subgrains. Narrower bands are bounded by parallel flakes of sericite. (c) Transmitted light photomicrograph (XPL). Deformation bands lying N–S in this relict quartz grain are cross-cut by NW–SE zones of subgrains and recrystallized grains. These lie at about 45° to the length of the relict grain and to the ribbons of recrystallized grains which surround it. (d) Reflected light photomicrograph (PPL) of an etched surface. The arrow points to a subgrain boundary in a relict grain (centre, N–S) which is surrounded by recrystallized grains. The black areas represent hollows, for many of the recrystallized grains fell out of this sample during the longer etch times required to reveal the subgrain structure. As in Fig. 3(b), the recrystallized grains and the subgrains are about the same size. The change in surface texture of the relict grain towards the top of the photograph represents a change in crystallographic orientation along its length.

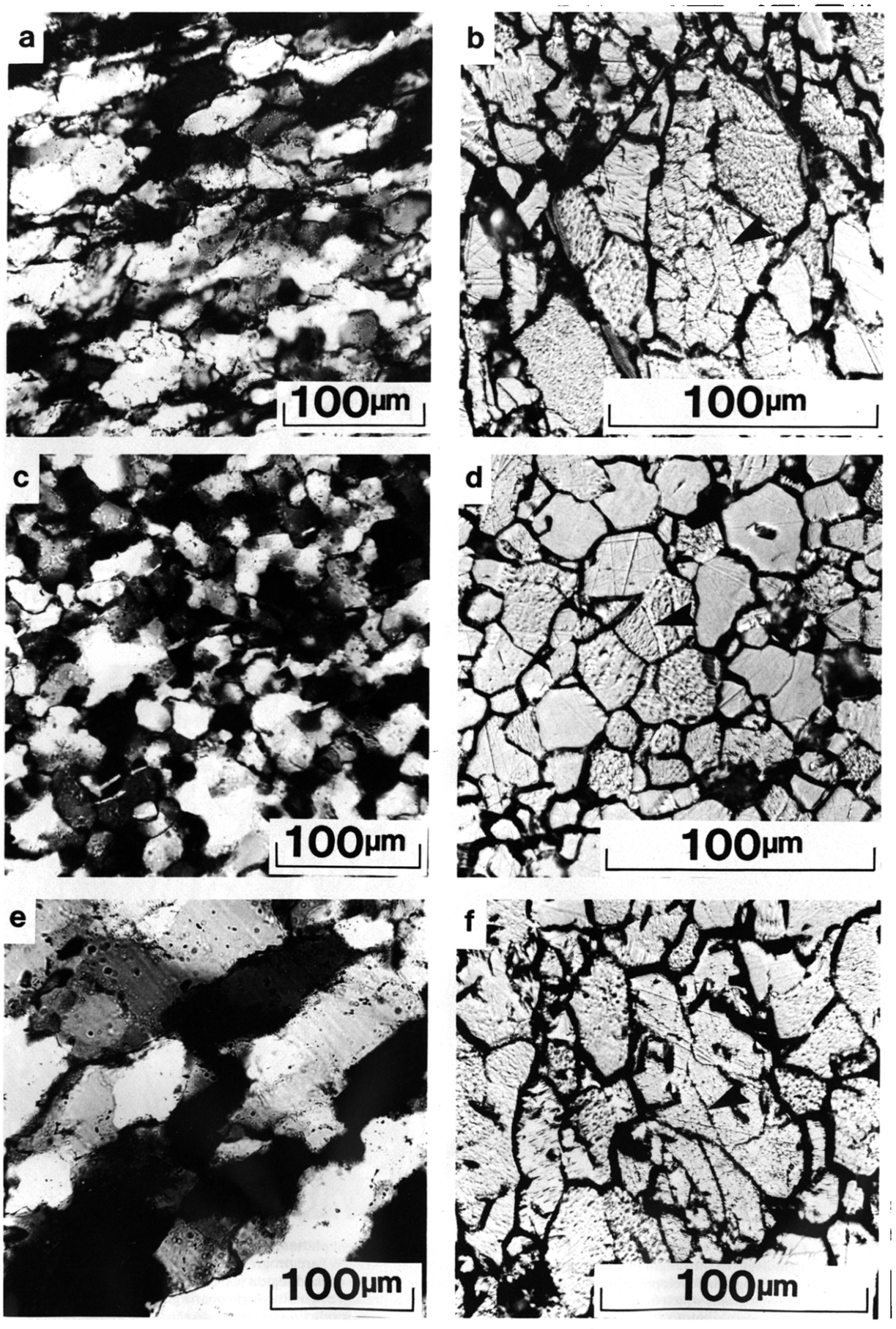

Fig. 5. Textures of recrystallized grains of deformed Type II quartzites in transmitted light (XPL) (left column) and in reflected light (PPL) (right column). Arrows in the right column point to subgrain boundaries in the larger recrystallized quartz grains. The different surface textures are the result of differential etching of the different crystallographic faces. (a) and (b) Specimen 4. The maximum grain elongation parallel to the foliation is shown best in XPL. The trace of the foliation trends approximately WSW–ENE. Subgrains in the larger recrystallized grains are half the size of the average recrystallized grain size (PPL). (c) and (d) Specimen 5. A few mica flakes are present at the quartz–quartz grain boundaries and are parallel to the mesoscopic foliation (SW–NE), ill-defined in this aggregate of equant recrystallized grains (XPL). The few subgrains present are also about half the size of the average recrystallized grains (PPL). (e) and (f) Specimen 6. These recrystallized grains (XPL) are elongate parallel to the trace of the foliation (SW–NE). The substructure present within the larger recrystallized grains is well defined by etching (PPL). The subgrain size is a third to a half of the recrystallized grain size.

The petrographic and microstructural characteristics of the samples are summarized in Table 1 and Figs. 2, 3, 4 and 5 which are best examined together. Figure 2 shows the microscopic and submicroscopic features of specimen 1, the foreland orthoquartzite. Dauphiné twinning is common in the rounded and undeformed quartz grains. Dislocations are generally tangled and may be associated with voids which presumably once contained some fluid phase. Minor recrystallization is present in specimen 2 (Fig. 3a) and is associated with deformation lamellae and subgrains, apparently mutually exclusive, in the elongate relict grains (Fig. 3b). Dislocation substructures are quite heterogeneous. The relationships between subgrains and recrystallized grains are best seen in specimen 3 (Fig. 4). The strong undulose extinction in the relict grains is seen to be a slightly misoriented subgrain structure, best revealed by etching (Fig. 4d). In some regions, recrystallized grains and subgrains may not be distinguished. Recrystallization is well developed in the necked regions of boudinaged relict quartz grains as well as in zones through the grains and at their boundaries. Recrystallization is complete in specimens 4, 5 and 6 (Fig. 5). The grains are elongate in specimens 4 and 6, and subgrains are present in the larger recrystallized grains.

Christie's Type I and Type II classification of these quartzites (Table 1, Christie 1963, pp. 397, 399) refers to their textures, the former "showing intense plastic deformation and granulation of grains" and the latter "showing post-kinematic recrystallization". The 'granulation' is inferred (Christie 1963, p. 405) to represent recrystallization. Similarities among individual diagrams of preferred crystallographic orientation for specimens of the quartzites of Types I and II, the primary mylonitic rocks (Christie 1960) and the Moine schists led Christie (1963, p. 402) to suggest that the quartz fabric in these rocks was induced during the same phase of the deformation. He suggested (p. 407) that movement during the final stages of the primary deformation was accompanied by recrystallization of quartz and feldspar. That is, that the microstructures formed by syntectonic recrystallization and should therefore reflect the flow stresses present during this period. The microstructures of specimen 5 may or may not reflect the late movement on the Ben More Thrust. This study examines the same specimens described by Christie to see if the history proposed earlier, or a more detailed one, could be distinguished from the microstructures.

The microstructural background required for interpretation of the microstructures will now be described before the main results are presented.

METHODS OF MICROSTRUCTURAL EXAMINATION

Subgrains and recrystallized grains

Thin sections were used for general petrographic examination of the textures of the rocks but not for measurement of subgrains or recrystallized grains. Subgrain and recrystallized grain dimensions were measured from reflected light photomicrographs of polished and etched slices with a thin reflecting coat of aluminium. TEM at magnifications of 5000–10,000 was used for measuring subgrain and recrystallized grain sizes up to 10 μm, thus overlapping with the range of grain sizes determined from etched surfaces.

The procedure for encapsulation, polishing and cleaning of specimens in preparation for etching is described by Wegner *et al.* (1978). The etching procedure is similar to that described for olivine (Wegner & Christie 1974) except for the composition of the etchant (40% NH_4HF_2; Wegner & Christie 1983). Recrystallized grain boundaries were clearly visible after an etch of 15 min, subgrain boundaries after 30–60 min. An alternating sequence of etching and measurement was used to measure grain and subgrain sizes.

Both the TEM and etching methods of measuring subgrain size have serious limitations. In both cases, the methods only permit observation and measurement of subgrains that are of the same order of size as the field of view at the magnifications employed. This results in subgrain diameters which are less than 7 μm at magnifications of greater than 10,000 in the electron microscope, and greater than 4 μm at magnifications of less than 700 in the optical microscope. In practice, subgrain sizes observed by optical microscopy are an order of magnitude larger than those observed by TEM. A high proportion of the small subgrain sizes sampled by TEM may be the tips of larger subgrains rather than one extreme of the subgrain sizes present in the sample. This dilemma may be partially resolved by comparing the average subgrain size observed by TEM to that observed by optical microscopy for a much larger sample size. TEM could also be used at an order of magnitude smaller magnification.

Also, in both cases, subgrain boundaries will not be resolved unless the dislocation spacing (h) is significantly less than the average dislocation spacing for the sample. The average dislocation density for these samples ranges from 10^8 to 10^9 cm^{-2}. These densities correspond to dislocation spacings of about 1–0.1 μm. If it is assumed that a dislocation spacing of 0.05 μm or less would be recognized as a subgrain boundary in TEM, then subgrains could be recognized which have a minimum misorientation of 0.6° [$\theta = b(\text{Å})/h(\text{Å})$; where b is the magnitude of the Burgers vector of the dislocation, taken here as 5Å and θ (radians; the angle of misorientation between subgrains) is small such that $\tan\theta = \theta$]. The situation is more complicated for subgrains revealed by etching.

Etch pits are not well resolved by optical microscopy unless their diameter is greater than 0.7 μm. Their sizes are dependent on the magnitude of the Burgers vector of the dislocation with which they are associated, the crystallographic orientation of the etch pit and its relation to the orientation of the etched surface, and the etching

Table 1. Specimen descriptions

Specimens *	Specimens Christie (1963) †	Classification	Recrystallized grains	Petrography
1 Figs. 2 (a–d)	—	Foreland orthoquartzite	None	Quartz grains, rounded, 0.1–1 mm diameter. Slight undulose extinction. Dauphiné twinning common. Deformation lamellae rare. Minor fractures
2 Figs. 3 (a–d)	X 17 p. 397 Pl. 8a ‡	Type I Quartzites (Christie 1963, pp. 400, 401)	<10%	Clastic quartz grains, flattened, with strong undulose extinction. Deformation lamellae, subgrains, Dauphiné twins common. Recrystallized quartz grains, common between relict grains and in zones cutting the foliation. Minor sericite between relict grains
3 Figs. 4 (a–d)	As 62 pp. 400, 401 Pl. 9 Fig. 23, D2 §		30%	Relict quartz grains, aspect ratio 100 : 10 : 1. Longest axis parallel to lineation; shortest axis normal to foliation. Grains up to 2 cm long. Deformation bands at slight angle to length of ribbon quartz. Few deformation lamellae in least strained relict grains. Minor sericite between grains.
4 Figs. 5 (a) & (b)	X 21 pp. 400, 401 Fig. 23, D4	Type II Quartzites (Christie 1963, pp. 400, 401)	100%	Quartz—strong dimensional orientation. Maximum grain elongation parallel to well-developed foliation. Impurities, mica and feldspar augen—fractured and boudinaged. Some feldspar recrystallized.
5 Figs. 5 (c) & (d)	As 55		100%	Equant grains display foam texture (Buiskool-Toxopeus 1977, p. 67). Mica flakes parallel to and pinning quartz–quartz grain boundaries.
6 Figs. 5 (e) & (f)	E 15 pp. 397, 400, 401 Pl. 8b Fig. 23, D9		100%	Dimensional orientation weak, slightly flattened in the foliation, elongate parallel to the lineation in the foliation. Random concentrations of mica flakes form closely spaced layers between quartz grains.

time. At dislocation densities of 10^8 to 10^9 cm^{-2}, the dislocation pits overlap. Then dislocation densities greater than 8×10^7 cm^{-2} may not be measured in this manner. When the etch pits are aligned, that line is recognized as a subgrain boundary. It is unlikely to be observed at a dislocation spacing greater than 0.1 μm, corresponding to a minimum misorientation of 0.3°. In practice, the misorientation is likely to be much larger such that boundaries of small misorientation are not resolved by etching and neither by optical observation nor by scanning electron microscopy.

The method used for measurement of subgrain and recrystallized grain size is that of lineal analysis (Smith & Guttmann 1953). This establishes a linear relationship between the number of intersections of grain boundaries with a random line passed through an aggregate, and the volumes of the grains. Its application to mylonites is described by Etheridge & Wilkie (1979), and by Christie & Ord (1980). This study assumes (after Christie & Ord 1980) that all the grains approximate cubes, so that the grain sizes quoted are $1.5\bar{N}_L$, where $\bar{N}_L$ is the mean linear intercept.

The recrystallized grain sizes were derived from an average of 1600 intercepts; the optically observed subgrain sizes from an average of 600 intercepts. The TEM measurements of subgrain sizes are averages of the longest and shortest dimensions of about 20 subgrains. In all cases, these are average values for each specimen.

A surface (~6 × 3 cm) of specimen 5, cut normal to the fold axis (B_n), was polished and etched. Recrystallized grain size measurements made parallel to as well as normal to the trace of the foliation on the surface of the sample were the same within one standard deviation from the mean. However, sericite is disseminated throughout this sample. The sizes measured were smaller by a third than those obtained for a different sample of the same specimen which was chosen for its high quartz content (Ord 1981, p. 22, fig. 1). Hence recrystallized grain size measurements were made in regions that were free from mica or other impurity phases, which limit the grain size by impeding the boundaries of quartz grains during growth (Hobbs 1966, Hobbs *et al.* 1976, pp. 112–113).

Dislocations

TEM of ion-thinned 'foils' was conducted on a JEOLCO model JEM-200 microscope fitted with a tilting stage with a tilt of 30 degrees and complete precession of the tilt axis, and with selected area diffraction.

The method used for calculating dislocation density for this study is that described by Schoeck (1962). The analysis is for a random spatial distribution of straight line dislocations without branching points, although

Table 1 (Continued)

Preferred crystallographic orientation of quartz *c*-axes	Microstructures: Subgrains—etched	Microstructures: Dislocation substructure
Not analysed in detail. Weak to absent.	Rare	Dislocations curved, frequently tangled. Triple nodes, small loops, irregular sub-boundaries, common—frequently associated with voids. Tangled boundaries separated by regions of much lower dislocation density resemble deformation lamellae. (McLaren *et al.* 1970, Ardell *et al.* 1976, McCormick 1977).
Deformation bands parallel *c*-axes. Weak preferred *c*-axis orientation. Strong preferred orientation of deformation lamellae—small circle girdle, radius 38° (Christie & Raleigh 1959).	Common in relict grains. Progressively misoriented outward from centres in zones parallel to deformation bands. Not observed in recrystallized grains.	Relict grains. Tangled dislocations. Dense tangles form cell boundaries. Ordered subgrain boundaries present. Voids common within, and at boundaries of cells. May form trails. Relict grain/recrystallized grain boundaries ill-defined at TEM magnifications. Dislocation substructures heterogeneous throughout. Recrystallized grains. Tangled and ordered dislocation arrays common. Dislocations curved and tangled. Loops, triple nodes, voids common.
Orthorhombic symmetry to *c*-axis orientations—relict, and larger recrystallized grains (optical analysis, Christie 1963). Overall monoclinic symmetry (X-ray analysis: Baker & Riekels 1977, Riekels & Baker 1977).		Qualitatively and quantitatively similar to specimens 4, 5 and 6.
Triclinic, trending toward orthorhombic symmetry of orientation diagrams.	Uncommon, but present in larger recrystallized grains.	Dislocations, straight and curved, are approximately evenly distributed.
Preferred orientation of quartz *c*-axes varies around fold.	Rare in recrystallized grains.	Loops, triple nodes, poor- to well-ordered subgrain boundaries common.
Almost orthorhombic symmetry of orientation diagrams. Regions of subgrains (of similar *c*-axis orientations) inferred to have formed from large single crystal pebbles (cf. Meilliez & Paquet 1979, p. 248)	Uncommon, but present in larger recrystallized grains.	Small (0.5–1 μm) voids within grains and at subgrain boundaries.

* Specimen numbers, figure references, this study.
† Specimen numbers, page and figure references, Christie (1963).
‡ Specimen IV, p. 395, Figs. 5 and 6, Christie & Raleigh (1959); Figs. 3(g) and 5(d), Carter *et al.* (1964) pp. 776, 777, Carter & Friedman (1965); figs. 8(c) & (d), Wegner & Christie (1982).
§ fig. 8(a), Wegner & Christie (1982).

Schoeck (1962, p. 1745) notes that the results apply also for closed loops and for random networks. The major error involved is considered to be that of invisibility of dislocations which may cause an underestimate of 30% (McCormick 1977).

An average of 3000 dislocations imaged in 30 TEM photographs at 10,000 to 20,000 times magnification was measured for each specimen.

Deformation lamellae

Deformation lamellae in relict quartz grains were tilted until parallel to the microscope axis. The lamellae were generally sub-basal. The lamellar spacing was measured on micrographs of these vertical planes by the intercept method. An average of 50 intercepts was counted on 8 grains per specimen.

PALEOPIEZOMETERS

The relationships of microstructure vs flow stress used in this study are described in this section. The data for recrystallized grain size, dislocation density and deformation lamellae spacing were derived from one suite of 'wet' experiments (Koch *et al.* 1980) not available to earlier workers who used microstructure vs flow stress relationships obtained from a variety of sources. It could therefore be assumed that the flow stresses derived from the natural microstructures would be consistent for each specimen if they formed during the one syntectonic recrystallization event. Conversely, if the flow stresses were inconsistent, more than one stress or temperature pulse could be inferred with greater confidence than in previous studies. Also, the microstructures in the specimens experimentally deformed under low differential stress are similar to those observed in the Assynt quartz mylonites. The primary mylonitic rocks from Assynt were deformed during prograde metamorphism to greenschist facies; the later secondary mylonitization may have been under greenschist or lower grade conditions (Christie 1960, p. 87, Christie 1963, p. 345). Such an environment is believed to have been simulated during the experiments as a result of the dehydration of the talc confining medium. Simpson quartzite was deformed in such hydrous assemblies in the alpha-quartz

Table 2. Paleopiezometers for quartz

(a) Recrystallized grain size (D, μm) σ(MPa) = AD^{-n}

A	n	Date	Reference
381	0.71	1977	Mercier *et al.*
603	0.68	1977	Twiss
4090	1.11	1980	Christie, Ord & Koch ('wet')
3902	1.43	1980	unpublished data ('dry')

(b) Subgrain size (d, μm) σ(MPa) = Bd^{-m}

B	m	Date	Reference
200	1	1977	Twiss

(c) Dislocation density (N, cm^{-2}) σ(MPa) = CN^{p}

C	p	Date	Reference
6.3×10^{-3}	0.5	1975	Goetze
1.64×10^{-4}	0.66	1977	McCormick (X-0 + X-13)
2.47×10^{-3}	0.5	1977	Twiss
6.6×10^{-3}	0.63	1979	Kohlstedt *et al.*
6.6×10^{-3}	0.5	1979	Weathers *et al.*
2.89×10^{-4}	0.67	1980	Kohlstedt & Weathers

(d) Deformation lamellae (s, μm) σ(MPa) = $D\,s^{-l}$

D	l	Date	Reference
3.65×10^{3}	2.18	1981	Koch & Christie ('wet' and 'dry')

field at temperatures of 750–900°C and strain rates of 10^{-4} s^{-1}–10^{-7} s^{-1} under a confining pressure of 1–1.2 GPa with differential stresses varying from 0.2 to 2.0 GPa (Koch *et al.* 1980). These experiments were also acknowledged by Sibson (1982, p. 157) as presently the most suitable for 'describing greenschist mylonitization of quartz-bearing rocks'.

Subgrains are scarce in recrystallized grains in the experimentally deformed material but are quite common in the relict grains where they are close in size to the surrounding recrystallized grains. However, they are not sufficiently developed for a subgrain size vs flow stress relationship to be confidently developed. Hence, a relationship between subgrain size and flow stress is used which is not derived from this suite of experiments. This relationship is described below together with a brief summary of all the microstructure vs flow stress relationships used recently in microstructural studies of quartz crystals and rocks (Table 2). These are dimensionally correct if A, B, C and D have dimensions of inverse stress and inverse scale of microstructure, and are of the form used in the literature of the past. The empirical relationships between stress and recrystallized grain and subgrain sizes and dislocation density are represented in Figs. 6 and 7, respectively.

Theoretical models for flow stress vs microstructural parameters have been derived by Holt (1970), Twiss (1977, 1980), Gittus (1979) and Edward *et al.* (1982). Physical constants in these models are still poorly constrained by existing experimental data. The models for quartz derived by Twiss (1977) are shown for comparison with the empirical relationships.

Recrystallized grain size

Mercier *et al.* (1977) derived an empirical relationship between flow stress and optically measured recrystallized grain size for quartzites.

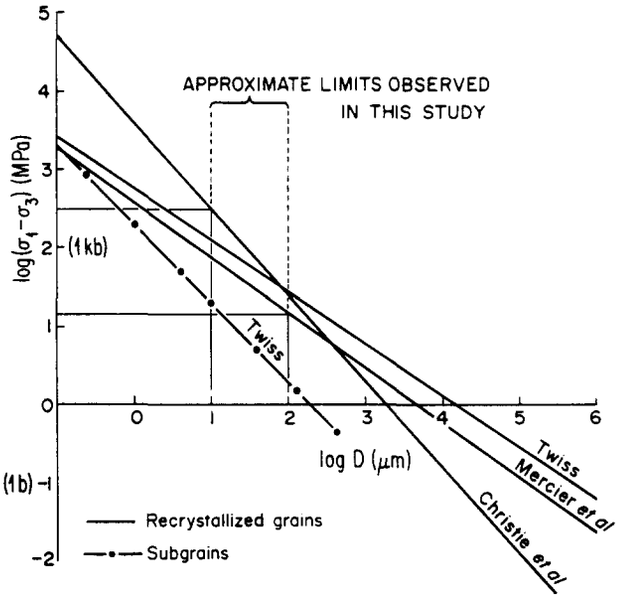

Fig. 6. Graph of equations relating the differential flow stress (σ_1–σ_3) (MPa) to the recrystallized grain size. D(μm), and to the subgrain size for quartz. Recrystallized grain sizes in the Assynt quartz mylonites range between 10 and 100 μm. Corresponding flow stresses range from 15 (Mercier *et al.* 1977) to 250 MPa (Christie *et al.* 1980).

We (Christie *et al.* 1980, unpublished data) have derived empirical relationships for flow stress vs recrystallized grain size for deformed Simpson quartzite. The relationship for the 'wet' experiments (Table 2, Fig. 6) will be used in the present work.

Subgrain size

There are no adequate experimental results relating subgrain size to flow stress in experimentally deformed quartzites. Hence, the only flow stress vs subgrain size relationship available for quartz, the theoretical one of Twiss (1977) (Table 2, Fig. 6), will be used in this study.

Dislocation density

The Weathers *et al.* (1979) relationship for dislocation density vs flow stress is based on a metallurgical model for work-hardening (Taylor 1934) with values for the different parameters based on Takeuchi & Argon (1976) together with a few data points for olivine, calcite and quartz. Kohlstedt & Weathers (1980) calculated the least-squares fit to a plot (Kohlstedt *et al.* 1979) of dislocation density vs flow stress for quartz (McCormick 1977) and for olivine (Kohlstedt & Goetze 1974, Durham *et al.* 1977, Zeuch & Green 1979).

The only empirically determined flow stress vs dislocation density relationship available for quartz is that of McCormick (1977). Recent measurements (Ord 1981, unpublished data) show that the free dislocation densities in recrystallized grains and subgrains in deformed Simpson quartzite are generally consistent with the equation derived by McCormick (1977) for single crystals deformed at lower stresses. Therefore, this equation is preferred in the present study (Table 2, Fig. 7).

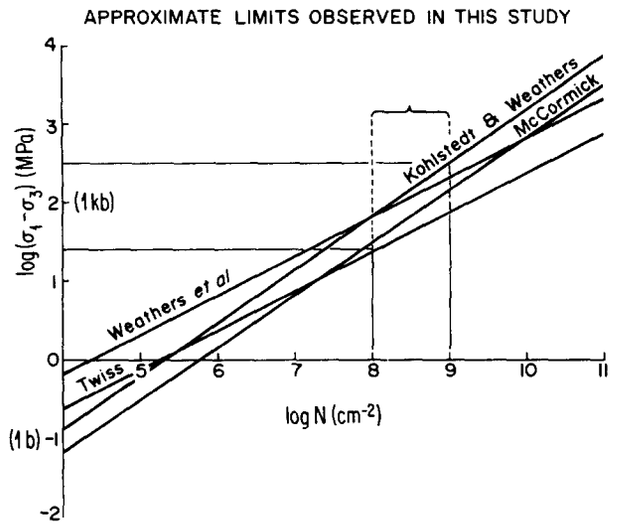

Fig. 7. Graph of equations relating the differential flow stress (σ_1–σ_3) (MPa) to dislocation density, N(cm^{-2}), for quartz. Dislocation densities in the Assynt mylonites range between 10^8 and 10^9 cm^{-2}. Corresponding flow stresses range from 20 (Twiss 1977) to 300 MPa (Kohlstedt & Weathers 1980).

Deformation lamellae

McCormick (1977, p. 43, fig. 33) recorded an inverse relationship between the spacing of prismatic deformation lamellae and the applied flow stress for synthetic quartz crystals deformed in creep. Koch and Christie (1981) have determined a similar relationship for the spacing of near-basal lamellae in deformed Simpson quartzite samples. This relationship (Table 2) will be used in the present study.

The much higher temperatures and faster strain rates in the experimentally deformed quartzites favour recrystallization whereas the lower temperatures and slower strain rates obtained in natural geologic settings favour recovery. The similarity of the microstructures in the naturally and the experimentally deformed specimens is consistent with the thesis that the deformation mechanisms active during experimental deformation are the same as those during natural deformation and that these are intra- rather than inter-crystalline processes.

MICROSTRUCTURES AND FLOW STRESSES

This work on the mylonitic quartzites from Assynt is the first for which paleostress analyses have been attempted on rocks which have already been studied and described in detail with respect to their structural and stratigraphic position (Christie 1963), their preferred orientation and textures (Christie 1963, Baker & Riekels 1977, Riekels & Baker 1977), and their microstructures (Christie & Raleigh 1959). The microstructural information increases that already available for the Moine Thrust from the earlier studies on specimens from other localities by White (1976), Kohlstedt *et al.* (1979) and Weathers *et al.* (1979). The full results of the microstructural studies described here are to be found in Tables 3–6, and will be summarized and interpreted below. These will then be compared with the results of Weathers *et al.* (1979) for the Stack of Glencoul, Loch Eriboll and Knockan Crag, and an interpretation made regarding plastic deformation and flow stresses along the Moine Thrust.

Table 3. Flow stresses (MPa) calculated from recrystallized grain sizes

Sample number	Recrystallized grain size (μm)	Inferred flow stress (MPa) Mercier *et al.* (1977)	Twiss (1977)	Christie *et al.* Unpublished data
2	12.7 ± 2.3	$62.7^{55.7}_{72.2}$	$107.1^{95.6}_{122.7}$	$243.5^{202.4}_{304.0}$
3	16.5 ± 2.3	$52.1^{47.5}_{57.9}$	$89.6^{82.0}_{99.3}$	$182.1^{157.5}_{215.1}$
4	34.6 ± 4.5	$30.8^{28.2}_{34.0}$	$54.2^{49.8}_{59.6}$	$80.0^{69.9}_{93.4}$
5	33.1 ± 5.1	$31.8^{28.7}_{35.8}$	$55.8^{50.6}_{62.6}$	$84.1^{71.7}_{101.2}$
6	61.2 ± 15.2	$20.5^{17.5}_{25.1}$	$36.8^{31.6}_{44.6}$	$42.5^{33.2}_{58.4}$
		Average	−1 standard deviation +1 standard deviation	

Table 4. Flow stresses (MPa) calculated from subgrain sizes

Sample number	Etched subgrain size (μm)	Flow stress Twiss (1977) (MPa)	TEM subgrain size (μm)	Flow stress Twiss (1977) (MPa)
2	19.7 ± 3.9 (relict grains)	$10.2^{8.5}_{12.7}$	2.6 ± 1.3 (all grains)	$76.9^{51.3}_{153.9}$
3	17.4 ± 3.7	$11.5^{9.5}_{14.6}$	2.7 ± 1.6	$74.1^{46.5}_{181.8}$
4	18.3 ± 5.5	$10.9^{8.4}_{15.6}$	2.1 ± 1.3	$95.2^{58.8}_{250.0}$
5	15.5 ± 5.0	$12.9^{9.8}_{19.0}$	3.5 ± 2.3	$57.1^{34.5}_{166.7}$
6	22.9 ± 7.2	$8.7^{6.6}_{12.7}$	4.0 ± 2.5	$50.0^{30.8}_{133.3}$
		Average	−1 standard deviation +1 standard deviation	

Table 5. Flow stresses (MPa) calculated from dislocation densities

Sample number	Dislocation density ($\times 10^8$ cm^{-2})	Inferred flow stress (MPa) McCormick (1977)	Twiss (1977)	Kohlstedt & Weathers (1980)
1	6.1 ± 2.7	—	—	—
2	10.4 ± 7.6	$146.6^{210.5}_{61.7}$	$79.7^{104.8}_{41.3}$	$317.9^{459.1}_{132.0}$
3	4.6 ± 2.4	$85.6^{112.9}_{52.6}$	$53.0^{65.4}_{36.6}$	$184.1^{243.8}_{112.3}$
4	4.1 ± 1.8	$79.3^{100.8}_{54.1}$	$50.0^{60.0}_{37.5}$	$170.4^{217.5}_{115.7}$
5	4.0 ± 2.8	$78.0^{110.7}_{35.2}$	$49.4^{64.4}_{27.1}$	$167.6^{239.2}_{74.8}$
6	3.8 ± 2.4	$75.4^{104.2}_{39.0}$	$48.1^{61.5}_{29.2}$	$161.9^{224.8}_{82.9}$
		Average	−1 standard deviation +1 standard deviation	

Table 6. Flow stresses (MPa) calculated from deformation lamellae

Sample number	Deformation lamellae spacing (μm)	Inferred flow stress Koch & Christie (1981) (MPa)
2	4.96 ± 1.61	$111.2^{60.3}_{261.6}$
	Average	−1 standard deviation +1 standard deviation

Results

The greatest variation is in the recrystallized grain sizes (Table 3). The Type I orthoquartzites have the smallest recrystallized grains, 13 μm for specimen 2 and 17 μm for specimen 3, which are smaller than the etched subgrains for each specimen, observed and measured only in relict grains. Of the Type II orthoquartzites, specimens 4 and 5 have about the same recrystallized grain sizes of 35 and 33 μm, respectively, double their subgrain size, while recrystallized grains in specimen 6, at 61 μm, are three times their etched subgrain size.

The subgrain sizes (Table 4) measured from polished and etched surfaces range from 15 to 23 μm whereas those measured in TEM range from 2 to 4 μm.

Dislocation densities for the recrystallized grains in the quartz mylonites (Table 5) are approximately constant at 4–5 $\times$ 10^8 cm^{-2}, with the exception of specimen 2 for which the dislocations are quite heterogeneous with an average density of 10 $\times$ 10^8 cm^{-2}. This value is also higher than that for the foreland orthoquartzite of 6 $\times$ 10^8 cm^{-2}.

The deformation lamellae spacing (Table 6) of specimen 2 is 5 μm, slightly larger than the TEM subgrain size.

Interpretation

The relative scales of the microstructures are of more use in interpreting different phases of deformation than flow stresses and shall therefore be used in this manner in the following discussion. However, the flow stresses derived using the empirical flow stress vs microstructure relationships for quartz will be used to indicate absolute values of flow stress for each phase. The microstructures will be interpreted with respect to the timing of dynamic recrystallization and/or recovery and annealing recrystallization and/or recovery.

The obvious associations are the almost constant values of subgrain size, measured by etching or by TEM methods, in both relict and recrystallized grains of the quartz mylonites, and the constancy of dislocation density. The recrystallized grain size varies between specimens but is always an integral multiple of the etched subgrain size. Specimen 2 is an anomaly and will be discussed separately.

It is immediately apparent that the dislocation density, subgrain size and recrystallized grain size were not formed during the same syntectonic recrystallization event for, in this case, dislocation density and subgrain size would be expected to vary with recrystallized grain size.

As a first case, consider the recrystallized grain size to be a product of dynamic recrystallization associated with an earlier event than that associated with the subgrain size and the dislocation density, and possibly forming simultaneously with the preferred orientations of quartz *c*-axes (Christie 1963, p. 402; Green *et al.* 1970, p. 328). In this case, there would have been two different stress pulses, and therefore only two values for flow stress may be inferred from the microstructures. It is clear that at least two interpretations of inferred flow stresses for the first event from the recrystallized grain sizes (Christie *et al.* unpublished data, Table 3 this study) are possible. The flow stresses are 182 MPa for specimen 3, 80 and 84 MPa for specimens 4 and 5, and 43 MPa for specimen 6. First, the flow stress may indeed have had these different values in different regions at the same time. Second, it is feasible that the flow stress was the same in the different regions but that the chemical environment was different, in which case the similar values for specimens 4 and 5 are fortuitous. The second event, dynamic recovery, resulted in the constant subgrain sizes and dislocation densities. This would be an unlikely result if the chemical environment of deformation was different for each of these specimens. A further problem with this interpretation is that the flow stresses inferred from optically measured subgrain sizes (Twiss 1977, Table 4 this study) range from 9 to 13 MPa whereas those inferred from dislocation densities (Fig. 8) and from recrystallized grain sizes (Fig. 9) range from 75 to 86 MPa (McCormick 1977, Table 5 this study) and from 43 to 182 MPa, respectively. This is inconsistent with observations for olivine and for rocksalt that indicate that subgrain size does not increase with decreasing stress and therefore reflects only the maximum stress (Ross *et al.* 1980, Friedman *et al.* 1981, Carter *et al.* 1982). The flow stresses of 50 to 95 MPa deduced from TEM subgrain sizes (Twiss 1977, Table 4 this study) are consistent with the dislocation density (Fig. 8) and therefore with the interpretation of two stress pulses but emphasize the need for an experimental study on the relationship of flow stress to subgrain size for quartz measured both optically and by TEM.

As a second case, again consider the dynamically recrystallized grain size to be the result of a first event, in this case followed by an annealing recovery event to give the observed subgrain development. The similar sizes

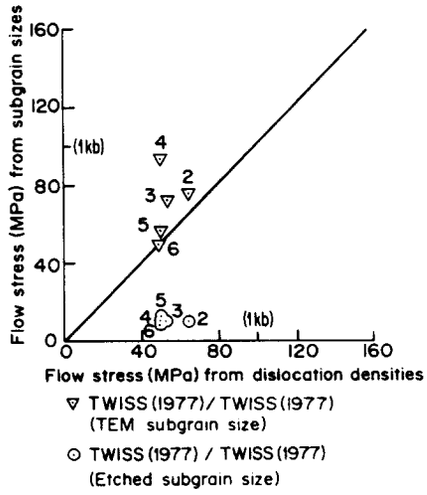

Fig. 8. Graph of flow stresses (MPa) estimated from dislocation densities (Twiss 1977) vs those estimated from subgrain sizes (Twiss 1977).

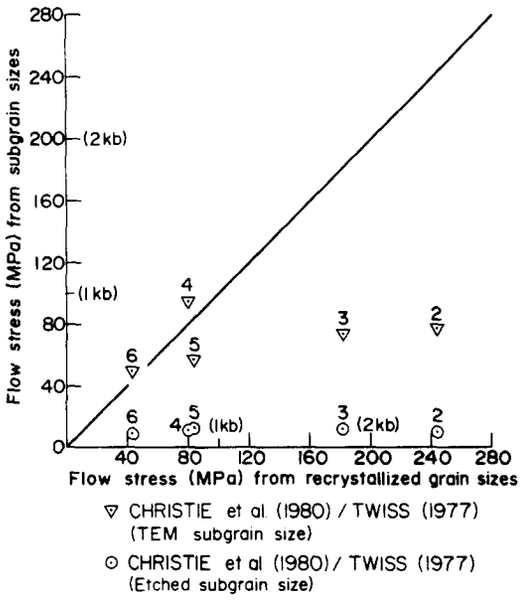

Fig. 9. Graph of flow stresses (MPa) estimated from recrystallized grain sizes (Christie *et al.* 1980) vs those estimated from subgrain sizes (Twiss 1977).

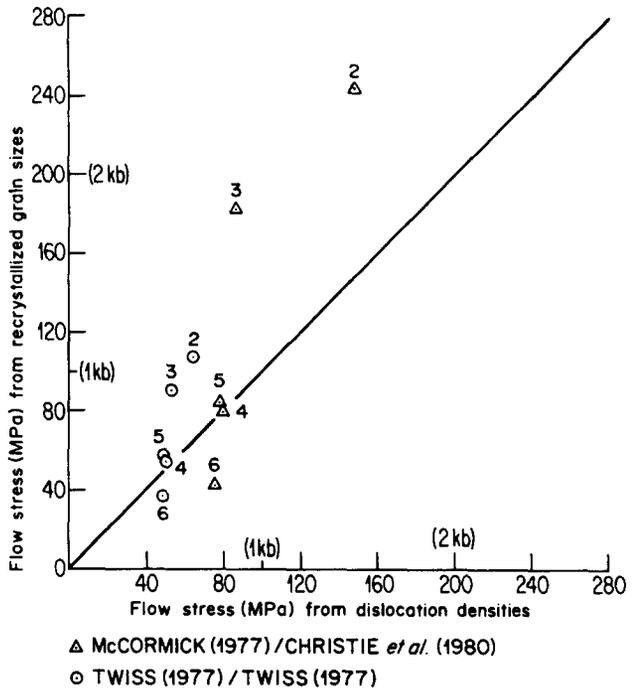

Fig. 10. Graph of flow stresses (MPa) estimated from dislocation densities (McCormick 1977, Twiss 1977) vs those estimated from recrystallized grain sizes (Christie *et al.* 1980, Twiss 1977).

for the subgrains could represent the one stress/temperature regime for the whole area. The dislocation densities could also be related to this recovery or they could reflect a further stress pulse. The inference from information available on other materials is that free dislocations are the least stable of the microstructures (see e.g. Jonas *et al.* 1969, McLaren & Hobbs 1972, pp. 63–64, Sandstrom & Lagneborg 1975, p. 389, Gueguen & Darot 1980) and are therefore first to respond to any changes in stress or temperature.

In the cases so far described, the recrystallized grain size has always been related to the flow stress. However, an annealing recrystallization event could be followed by late dynamic recovery so that subgrain size represents flow stress. Again, dislocation density may represent the latter flow stress or some later event (see Fig. 10).

The final option is that a late annealing recovery and recrystallization event occurs such that none of the microstructures are related to flow stress and the preferred orientation from an earlier event either remains, is strengthened, or is changed. However, the temperatures in this region may not have been sufficiently high for significant annealing to have occurred (Christie & Ord 1980, p. 6261). None of the microstructures seem to have been affected by the even later folding event which resulted in the rotation of *c*-axes around the B_n fold axis in specimen 5.

Specimen 2 has subgrains in the relict grains which are larger than the recrystallized grains, and a high dislocation density. An initial high stress event (244 MPa from recrystallized grain size) resulting in the preferred *c*-axis orientations in the relict grains followed by a lower stress, dynamic recovery event (10 MPa from etched subgrain size, 77 MPa from TEM subgrain size) and a later high stress pulse (147 MPa from dislocation density, 111 MPa from deformation lamellae) may account for this structure. It is consistent with the interpretation of Christie & Raleigh (1959) that the lamellae dated from a late stage in the deformation of the rock and were unrelated to the deformation which produced the crystallographic preferred orientations of the quartz grains. The similar values from deformation lamellae and dislocations are consistent with the formation of deformation lamellae being directly related to the dislocation density. However, it is still inconsistent with subgrain size reflecting the maximum stress.

This summarizes the information to be obtained from this study. The next section will compare the results of this study with an earlier study which was conducted in this region and which concentrated on the change in recrystallized grain size and dislocation density with progressive mylonitization. Weathers *et al.* (1979) sampled the basal quartzite along a traverse normal to its contact with the Moine Schist at the Stack of Glencoul, out to approximately 110 m into the quartzite unit. They observed all the petrographic features described by Christie (1963), which are those described earlier in this study. They observed dislocation density to be independent of distance from the fault, averaging 4×10^8 cm^{-2}, and 5×10^8 cm^{-2} in the overthrust schist, and an average spacing for TEM-scale cells or subgrains to be 2 μm, similar to the results obtained in this study. They did not measure deformation lamellae spacing, nor subgrain sizes from etched surfaces. The recrystallized grain sizes they measured from thin sections were found to range from 10 to 20 μm, averaging 15 μm, as for specimens 2 and 3 of this study and collected from the same region. They also examined the quartzite at Loch Eriboll (Fig. 1, insert), about 50 km NNE of the Stack where Lewisian Gneiss has been thrust over the basal quartzite, and noted an average dislocation density

of about 2.5×10^8 cm^{-2} on either side of the fault surface, and an average recrystallized grain size of 20 μm. A third study was conducted at Knockan Crag, at the SW corner of the 'Assynt bulge' (Fig. 1), where the Moine Schists directly overlie the Cambrian Durness Limestone. The dislocation density in quartz grains of the Moine Schists was again found to be independent of distance from the fault and to average $8–10 \times 10^8$ cm^{-2} (Weathers *et al.* 1979, fig. 9, Table 1). Weathers *et al.* found the recrystallized grain size in the Moine Schists at Knockan Crag and at the Stack of Glencoul to vary between 10 and 50 μm, being slightly finer in the more deformed material. However, this information is not used in their discussion. They did not observe the larger recrystallized grain sizes of about 30 and 60 μm found in the present study in the basal quartzite. The differences in data and interpretation will be discussed in the following section.

It may be inferred that the average recrystallized grain size of 10–20 μm at or near the Stack of Glencoul, as in specimens 2 and 3 of this study and in the specimens of Weathers *et al.* (1979), does correspond to the flow stress during the progressive mylonitization, which would then be between 318 and 147 MPa (Christie *et al.* unpublished data) or between 126 and 79 MPa (Twiss 1977). The latter values are consistent with the 100 MPa (Twiss 1977) noted by Etheridge & Wilkie (1981) for mylonite zones of different geometries and tectonic settings. However, the higher values derived using the experimentally determined relationships are preferred. If the recrystallized grain sizes in our specimens 4, 5 and 6 represent the flow stresses during the same event, then they decrease to the east and to the south of the Stack. This is at odds with the conclusion of Weathers *et al.* (1979, p. 1506) that the differential stress decreases as one goes north from Knockan Crag to Loch Eriboll. We consider that the complexity of results which we have obtained from five now extremely well-characterized quartz mylonites makes such an interpretation invalid.

SUMMARY AND DISCUSSION

This analysis of the relative times of formation of different microstructures in one suite of rocks and the flow stresses derived from them shows more strongly than previous studies the lack of information on, and understanding of, recrystallization and recovery processes in quartzites. Most immediately felt in this study was the lack of experimental information on subgrain size vs flow stress. The following interpretation of the stress and temperature pulses represented by the microstructural information obtained from the Assynt region is made assuming subgrain size to represent the same flow stress as dislocation density.

The results of this study are compatible with a range in the flow stress from 202 MPa, derived from an average recrystallized grain size of 15 μm associated with the progressive mylonitization at the Stack of Glencoul, to 43 MPa (60 μm) in the recrystallized quartzite lens represented by specimen 6. The formation of the quartz fabrics may have been associated with this syntectonic recrystallization event. A late annealing recovery event affecting the whole region fixed the subgrain size at 15 μm (etched) and 3 μm (TEM), and the dislocation density at $4–10 \times 10^8$ cm^{-2}. However, the flow stress inferred from dislocation density for specimen 6 is higher than that inferred from its recrystallized grain size, possibly as a result of some later stress pulse during the incorporation of the quartzite lens into the primary mylonitic rocks. On the other hand, the folding associated with the late movement on the Ben More Thrust does not seem to have affected the microstructures of specimen 5.

Obviously, the microstructures of rocks from different regions along the Moine Thrust reflect neither a simple history nor the same history, which is to be expected from the long and complex structural and thermal history which the rocks associated with the Moine Thrust have undergone (see McClay & Coward 1981, for the most recent review).

A more detailed interpretation of the microstructures described in this study will be possible when further experimental information on the behaviour of quartz and quartzites during deformation becomes available.

It is well known that the addition of water strongly affects the strength of quartz (Griggs & Blacic 1964, 1965), the kinetics and mechanisms of recrystallization, recovery and grain growth in deformed and undeformed quartz aggregates (Green *et al.* 1970, Cooper & Kohlstedt 1979, Tullis & Yund 1982) and the microstructure vs flow stress relationships (Bell & Etheridge 1976, Christie *et al.* 1980). However, there have been no complete quantitative experimental studies on the effects of annealing recovery and annealing recrystallization on the relative rates of change of the magnitudes of the various microstructures and on the behaviour of different patterns of preferred orientations produced during deformation (Hobbs 1968, Green *et al.* 1970, and see Hobbs *et al.* 1976, pp. 135–140 for a brief review). The presence of other impurities may also affect the recrystallization and recovery processes (Hobbs 1981, 1983, Etheridge & Wilkie 1981, Edward *et al.* 1982, Jaoul 1983) and the flow stress vs microstructure relationships (Knipe 1980). Although Tullis & Yund (1982) concluded that grain growth rates would only be substantially diminished by impurities which were insoluble in the intergranular fluid and would therefore affect inter- rather than intra-crystalline deformation processes, Jaoul (1983) interpreted the decreased strength of Heavitree quartzite doped with sodium with respect to equivalent undoped specimens to be a result of enhanced dislocation glide. Initial studies also display a dependence of the flow strength of quartz upon its chemical environment during deformation (Hobbs 1983, Ord & Hobbs 1983).

A change in the initial grain size of the specimens used in experimental deformation studies causes a slight vari-

ation in the flow stress vs microstructure relationships for quartz. Recrystallized grain sizes for Arkansas novaculite (original grain size, 7 μm) (Christie & Koch 1982) are similar to those derived from 'wet' Simpson quartzite (original grain size, 210 μm) (Christie *et al.* 1980) in the lower half of the stress range but are larger in the novaculite at higher stresses. The novaculite was also shown to be stronger than the Simpson quartzite and showed no mechanical evidence for superplasticity (Koch & Christie 1982).

These examples emphasize the uncertainties present in the derivation of flow stresses from microstructural information, but they also emphasize the power of this technique when such information becomes available.

CONCLUSIONS

Flow stresses ranging from 43 to 202 MPa are represented by dynamically recrystallized grain sizes of quartz mylonites from the basal quartzite unit associated with the Moine Thrust in the region of the 'Assynt bulge' for the same event represented by the preferred orientations of quartz *c*-axes for the same specimens. A late annealing recovery event resulted in a constant subgrain size and dislocation density for all the specimens. The history is probably more complex than this but will not be determined until experimental information becomes available for subgrain size, at all magnifications, vs flow stress. Further, experiments should be conducted under a controlled chemical environment so that the results may be more rigorously applied to naturally deformed rocks.

This study shows that all microstructures available for examination in a rock should be studied before a detailed interpretation may be made of the stress and temperature pulses which affected that rock. Paleopiezometers are an extremely powerful tool for determining such detailed histories as well as the stress magnitudes during deformation.

Note added in proof: Since this paper was submitted for publication, a doctoral dissertation has been presented to the University of California at Los Angeles by Philip S. Koch, entitled Rheology and Microstructures of Experimentally Deformed Quartz Aggregates. The three conclusions of this thesis which differ from information used in this paper are that a microstructure–flow stress relationship may be determined from etched subgrain size but not from dislocation density, and that none of the derived relationships appear to depend upon initial grain size, nor even upon 'wetness'. The ranges of flow stresses obtained for the Assynt specimens using the empirical relationships described in this thesis are 34–488 MPa from recrystallized grain size, 27–57 MPa from etched subgrain size and 76 MPa from deformation lamellae spacing. Flow stresses inferred from etched subgrains are still lower than those inferred from any other microstructure.

Acknowledgements—Assistance from M. W. Wegner is gratefully acknowledged. B. E. Hobbs and M. A. Etheridge provided useful comments on the manuscript. J. de Grosse prepared the doubly-polished sections and the polished quartzite specimens. This work was supported in part by NSF grant EAR 77-23163. A.O. acknowledges the financial support provided by U.C.L.A. during her post-graduate studies.

REFERENCES

Ardell, A. J., Christie, J. M., Kirby, S. H. & McCormick, J. W. 1976. Electron microscopy of deformation structures in quartz. In: *Developments in Electron Microscopy and Analysis* (edited by Venables, J. A.). Academic Press, London, 467–470.

Baker, D. W. & Riekels, L. M. 1977. Dauphiné twinning in quartzite mylonite. *J. Geol.* **85**, 15–26.

Bell, T. H. & Etheridge, M. A. 1976. The deformation and recrystallization of quartz in a mylonite zone, Central Australia. *Tectonophysics* **32**, 234–267.

Bird, J. E., Mukherjee, A. K. & Dorn, J. F. 1969. Correlations between high temperature creep behaviour and structure. In: *Quantitative Relation between Properties and Microstructure* (edited by Brandon, D. G. & Rosen, R.). Israel Universities Press, Jerusalem, 255–342.

Buiskool-Toxopeus, J. M. A. 1977. Fabric development of olivine in a peridotite mylonite. *Tectonophysics* **39**, 55–71.

Carter, N. L. & Friedman, M. 1965. Dynamic analysis of deformed quartz and calcite from the Dry Creek Ridge anticline, Montana. *Am. J. Sci.* **263**, 747—785.

Carter, N. L., Christie, J. M. & Griggs, D. T. 1964. Experimental deformation and recrystallization of quartz. *J. Geol.* **72**, 687–733.

Carter, N. L., Hansen, F. D. & Senseny, P. E. 1982. Stress magnitudes in natural rock salt. *J. geophys. Res.* **87**, 9289–9300.

Christie, J. M. 1960. Mylonitic rocks of the Moine Thrust-Zone in the Assynt region, NW Scotland. *Trans. geol. Soc. Edinb.* **18**, 79–93.

Christie, J. M. 1963. The Moine Thrust Zone in the Assynt region, NW Scotland. *Univ. Calif. Publs geol. Sci.* **40**, 345–439.

Christie, J. M. & Koch, P. S. 1982. Grain size-flow stress relations for novaculite deformed in hydrous assemblies. *EOS Trans. Am. geophys. Un.* **63**, 1095.

Christie, J. M. & Ord, A. 1980. Flow stress from microstructures of mylonites: example and current assessment. *J. geophys. Res.* **85**, 6253–6262.

Christie, J. M. & Raleigh, C. B. 1959. The origin of deformation lamellae in quartz. *Am. J. Sci.* **257**, 385–407.

Christie, J. M., Ord, A. & Koch, P. S. 1980. Relationship between recrystallized grain size and flow stress in experimentally deformed quartzite (abstract). *EOS Trans. Am. geophys. Un.* **61**, 377.

Cooper, R. F. & Kohlstedt, D. L. 1979. Dislocation recovery in naturally deformed quartz (abstract). *EOS Trans. Am. geophys. Un.* **60**, 370.

Durham, W. B., Goetze, C. & Blake, B. 1977. Plastic flow of oriented single crystals of olivine, Part II. *J. geophys. Res.* **82**, 5755–5770.

Edward, G. H., Etheridge, M. A. & Hobbs, B. E. 1982. On the stress dependence of subgrain size. *Textures and Microstructures* **5**, 127–152.

Elliott, D. & Johnson, M. R. W. 1980. Structural evolution in the Moine thrust belt, NW Scotland. *Trans. R. Soc. Edinb.: Earth Sci.* **71**, 69–96.

Etheridge, M. A. & Wilkie, J. C. 1979. The geometry and microstructure of a range of QP-mylonite zones: a field test of the recrystallized grain size palaeopiezometer. *Analysis of Actual Fault Zones in Bedrock*, 448–504, Open File Report 79-1239, U.S. Geol. Surv., Menlo Park, Calif.

Etheridge, M. A. & Wilkie, J. C. 1981. An assessment of dynamically recrystallized grain size as a palaeopiezometer in quartz-bearing mylonite zones. *Tectonophysics* **78**, 475–508.

Friedman, M., Dula, W. F., Gangi, A. F. & Gazonas, G. A. 1981. Subgrain size vs stress in experimentally deformed synthetic rocksalt (abstract). *EOS Trans. Am. geophys. Un.* **62**, 397.

Gittus, J. H. 1979. Theoretical relationship between free energy and dislocation cell diameter during creep. *Phil. Mag.* **A39**, 829–832.

Goetze, C. 1975. Sheared lherzolites: from the point of view of rock mechanics. *Geology* **3**, 172–173.

Green, H. W., Griggs, D. T. & Christie, J. M. 1970. Syntectonic and annealing recrystallization of fine-grained quartz aggregates. In: *Experimental and Natural Rock Deformation* (edited by Paulitsch, P.). Springer, Berlin, 272–335.

Griggs, D. T. & Blacic, J. D. 1964. The strength of quartz in the ductile regime (abstract). *EOS Trans. Am. geophys. Un.* **45**, 102–103.

Griggs, D. T. & Blacic, J. D. 1965. Quartz: anomalous weakness of synthetic crystals. *Science, Wash.* **147**, 292.

Gueguen, Y. & Darot, M. 1980. Microstructures and stresses in naturally deformed peridotites. *Rock Mech. (Suppl.)* **9**, 159–172.

Hobbs, B. E. 1966. Microfabric of tectonites from the Wyangala Dam area, New South Wales, Australia. *Bull. geol. Soc. Am.* **77**, 685–706.

Hobbs, B. E. 1968. Recrystallization of single crystals of quartz. *Tectonophysics* **6**, 353–401.

Hobbs, B. E. 1981. The influence of metamorphic environment upon the deformation of minerals. *Tectonophysics* **78**, 335–383.

Hobbs, B. E. in press. The hydrolytic weakening effect in quartz. *J. geophys. Res.*

Hobbs, B. E., Means, W. D. & Williams, P. F. 1976. *An Outline of Structural Geology*. John Wiley, New York.

Holt, D. L. 1970. Dislocation cell formation in metals. *J. appl. Phys.* **41**, 3197–3201.

Jaoul, O. in press. Sodium weakening of Heavitree Quartzite. *J. geophys. Res.*

Jonas, J. J., Sellars, C. M. & Tegart, W. J. McG. 1969. Strength and structure under hot-working conditions. *Metal. Rev.* **14**, 1–24.

Knipe, R. J. 1980. Distribution of impurities in deformed quartz and its implications for deformation studies. *Tectonophysics* **64**, T11–T18.

Koch, P. S. & Christie, J. M. 1981. Spacing of deformation lamellae as a paleopiezometer (abstract). *EOS Trans. Am. geophys. Un.* **62**, 1030.

Koch, P. S. & Christie, J. M. 1982. High-temperature flow law of Arkansas novaculite in the α-quartz field. *EOS Trans. Am. geophys. Un.* **63**, 1095.

Koch, P. S., Christie, J. M. & George, R. P. 1980. Flow law of 'wet' quartzite in the α-quartz field (abstract). *EOS Trans. Am. geophys. Un.* **61**, 376.

Kohlstedt, D. L. & Goetze, C. 1974. Low-stress high-temperature creep in olivine single crystals. *J. geophys. Res.* **79**, 2045–2051.

Kohlstedt, D. L. & Weathers, M. S. 1980. Deformation-induced microstructures, paleopiezometers, and differential stresses in deeply eroded fault zones. *J. geophys. Res.* **85**, 6269–6285.

Kohlstedt, D. L., Cooper, R. F., Weathers, M. S. & Bird, J. M. 1979. Paleostress analysis of deformation-induced microstructures: Moine Thrust Zone and Ikertoq shear zone. *Analysis of Actual Fault Zones in Bedrock*, 394–425, Open File Report 79-1239, U.S. Geol. Surv., Menlo Park, Calif.

McClay, K. R. & Coward, M. P. 1981. The Moine Thrust Zone: an overview. In: *Thrust and Nappe Tectonics* (edited by McClay, K. R. & Price, N. J.). Blackwell, Oxford, 241–260.

McCormick, J. W. 1977. Transmission electron microscopy of experimentally deformed synthetic quartz. Unpublished Ph.D thesis, University of California, Los Angeles.

McLaren, A. C. & Hobbs, B. E. 1972. Transmission electron microscope investigation of some naturally deformed quartzites. *Am. geophys. Un. Geophys. Monogr.* **16**, 55–66.

McLaren, A. C., Turner, R. G., Boland, J. N. & Hobbs, B. E. 1970. Dislocation structure of the deformation lamellae in synthetic quartz; a study by electron and optical microscopy. *Contr. Miner. Petrol.* **29**, 104–115.

McQueen, H. J. & Jonas, J. J. 1975. Recovery and recrystallization during high temperature deformation. In: *Treatise on Materials Science and Technology*, **6**, *Plastic Deformation of Materials* (edited by Arsenault, R. J.). Academic Press, San Francisco, 393–493.

Meilliez, F. & Paquet, J. 1979. Microtextures de grains de quartz d'une tectonite quartzo-feldspathique: signification. *Bull. Mineral.* **102**, 242–248.

Mercier, J.-C., Anderson, D. A. & Carter, N. L. 1977. Stress in the lithosphere: inferences from steady-state flow of rocks. *Pure appl. Geophys.* **115**, 199–226.

Ord, A. 1981. Determination of flow stress from microstructures of mylonitic rocks. Unpublished Ph.D. thesis, University of California, Los Angeles.

Ord, A. & Hobbs, B. E. 1983. Oxygen dependence of the hydrolytic weakening effect in quartz. *EOS Trans. Am. geophys. Un.* **64**, 839.

Paterson, M. S. & Kekulawala, K. R. S. S. 1979. The role of water in quartz deformation. *Bull. Mineral.* **102**, 92–98.

Peach, B. N., Horne, J., Gunn, W., Clough, C. T., Hinxman, L. W. & Teall, J. J. H. 1907. The geological structure of the north-west Highlands of Scotland. *Mem. geol. Surv. Gt. Brit.*

Riekels, L. M. & Baker, D. W. 1977. The origin of the double maximum pattern of optic axis in quartzite mylonite. *J. Geol.* **85**, 1–14.

Ross, J. V., Avé Lallemant, H. G. & Carter, N. L. 1980. Stress dependence of recrystallized-grain and subgrain size in olivine. *Tectonophysics* **70**, 39–61.

Sandstrom, R. & Lagneborg, R. 1975. A model for hot working occurring by recrystallization. *Acta Metall.* **23**, 387–398.

Schoeck, G. 1962. Correlation between dislocation length and density. *J. appl. Phys.* **33**, 1745–1747.

Sibson, R. H. 1982. Fault zone models, heat flow, and the depth distribution of earthquakes in the continental crust of the United States. *Bull. seism. Soc. Am.* **72**, 151–163.

Smith, C. S. & Guttman, L. 1953. Measurement of internal boundaries in three-dimensional structures by random sectioning. *Trans. AIME* **197**, 81–87.

Takeuchi, S. & Argon, A. S. 1976. Review: Steady state creep of single-phase crystalline matter at high temperatures. *J. Mater. Sci.* **11**, 1542–1566.

Taylor, G. I. 1934. The mechanism of plastic deformation of crystals, Part I: theoretical. *Proc. R. Soc.* **A145**, 362–387.

Tullis, J. & Yund, R. A. 1982. Grain growth kinetics of quartz and calcite aggregates. *J. Geol.* **90**, 301–318.

Twiss, R. J. 1977. Theory and applicability of a recrystallized grain size paleopiezometer. *Pure appl. Geophys.* **115**, 227–244.

Twiss, R. J. 1980. Static theory of size variation with stress for subgrains and dynamically recrystallized grains. In: *Proc. Conf. IX, Magnitude of Deviatoric Stresses in the Earth's Crust and Upper Mantle*, 665–683, Open File Report 80-625, U.S. Geol. Surv., Menlo Park, Calif.

Weathers, M. S., Bird, J. M., Cooper, R. F. & Kohlstedt, D. L. 1979. Differential stress determined from deformation-induced microstructures of the Moine Thrust Zone. *J. geophys. Res.* **84**, 7495–7509.

Wegner, M. W. & Christie, J. M. 1974. Preferential chemical etching of terrestrial and lunar olivines. *Contr. Miner. Petrol.* **43**, 195–212.

Wegner, M. W. & Christie, J. M. 1983. Chemical etching of deformation sub-structures in quartz. *Phys. Chem. Minerals* **9**, 67–78.

Wegner, M. W., Jones, R. E. & Christie, J. M. 1978. Exsolution in terrestrial and lunar plagioclases revealed by chemical etching. *Contr. Miner. Petrol.* **65**, 283–291.

White, S. 1976. The determination of deformation parameters from dislocation sub-structures in naturally deformed quartz. In: *Developments in Electron Microscopy and Analysis* (edited by Venables, J. A.). Academic Press, London, 505–508.

Zeuch, D. H. & Green, H. W. 1979. Experimental deformation of an 'anhydrous' synthetic dunite. *Bull. Mineral.* **102**, 185–187.